The Field-Assisted Stepwise Dissociation of Acetone in an Intense Femtosecond Laser Field

Xiao-ping Tang, Su-fan Wang, Mohamed E. Elshakre,† Li-rong Gao, Yong-ling Wang, Hong-fei Wang, and Fan-ao Kong*

State Key Laboratory of Molecular Reaction Dynamics, Center for Molecular Sciences Institute of Chemistry, Chinese Academy of Sciences, Beijing 100080, China

Received: June 19, 2002; In Final Form: October 21, 2002

The dissociation of acetone in an intense ($10^{13}-10^{14}$ W/cm^2) femtosecond laser field has been investigated. The stepwise nature of the dissociation has been verified by analyzing the time-of-flight mass spectroscopic patterns at different laser intensities. The stepwise nature was interpreted using a quasi-diatomic field-assisted dissociation model and the QCT calculations. Both the experimental identification and the theoretical predictions show that if the laser intensity is gradually increased, the sequence of the primary dissociation is C−C, C−O, and C−H bonds in the acetone ion. The preference of breaking the C−C and C−O bond over the H-elimination of the C−H bond is also the case in the secondary dissociation.

I. Introduction

Intense laser fields can readily be achieved using ultrashort lasers pulses, which can be generated from tabletop Ti:sapphire lasers. The imposed E-fields of such laser pulses on a molecule are as strong as the internal fields that bind the outer electrons in atoms and molecules. It is possible now, if a 100 fs laser pulse is focused to a diameter of 60 μm, to produce average intensity of such a pulse reaching the tens of petawatts range (about 35×10^{15} W/cm^2), and the corresponding electric field associated with such laser light is equal to the Coulomb field binding the ground-state electron in a hydrogen atom. Such intense laser field effects on atoms and molecules attracted and continue to attract considerable interest.[1−5] The effects on molecules by the electric field present in intense light fields give rise to several phenomena, which have major consequences on the dynamics of molecular dissociation and ionization. A few to mention of these phenomena are above threshold dissociation (ATD),[4] bond softening,[6] vibrational trapping,[7] Coulomb explosion,[8−11] molecular alignment,[12−15] and dissociative ionization.[1−5]A few studies had been reported by Cornaggia and co-workers,[16−19] Mathur and co-workers,[20−23] Castillejo and co-workers,[24,25] Ledingham and co-workers,[26−30] and Wu et al.[31] on the dynamical behavior of polyatomic molecules. Among these new phenomena, chemists are more interested in the dissociation of molecules caused by strong laser field. Many studies have been performed on the dissociative ionization of diatomic[16,19,32] and triatomic molecules.[16,18−19,32,33−40] For polyatomic molecules, unfortunately, there has been a lack of careful experimental investigations, as well as adequate dynamic theory. The only theory that has been widely used to interpret the dissociation of polyatomic molecules is the Coulomb explosion model. The model is based on the assumption that fragmentation of a multiply charged polyatomic molecular ion may take place driven by the Coulombic repulsive forces, yielding the smaller fragmented ions. The model can interpret the dissociation of the molecular ions at very high laser intensities ($10^{14}-10^{16}$ W/cm^2) at which the multiply charged molecular ions are readily formed. However, at the moderate laser intensities of $10^{13}-10^{14}$ W/cm^2, the applied E-field only produces singly charged molecular ions. The field-assisted dissociation of the molecular ions may take place in a stepwise manner. Therefore, cracking of the chemical bond in the intense laser field should be considered from a different point of view.

There are several reasons that acetone was chosen for such intense field dissociation. Acetone is a typical molecule for the conventional photodissociation in weak field and is considered the most elementary ketone. Its photochemistry including its photodissociation in the α-bond cleavage has been of considerable interest and has been extensively investigated.[43−62] Acetone undergoes Norrish type-I reactions,[63] which have been the most extensively investigated areas in photochemistry.[48] Such reactions have provided good model systems to address some important issues in photochemistry such as dissociation mechanisms.[45,64] A primary issue in previous studies, especially for dissociation at 193 nm, was whether the dissociation of the two C−C bonds is concerted (simultaneous) or stepwise (sequential). Through a combination of product studies and ultrafast spectroscopy, it has been demonstrated that for all of the electronically excited states, Lee,[60] Zewail,[61] Leone,[48,58] and Baronavski,[65] dissociation takes place in a stepwise manner. However, fundamental issues concerning the photodissociation of acetone are still unresolved. Kong and co-workers[66] studied the photolysis using time-resolved FTIR for detecting the CO emission resulting from the UV photolysis. Their results showed that the CO emission is power-dependent. Acetone absorbs the first 248 or 266 nm photon, which yields an acetyl radical, CH_3CO, and the acetyl radical absorbs another photon, producing the hot CO fragment. However, a fast photodissociation of acetone will directly yield CO, if the molecule absorbs a 193 nm photon.

Recently, the investigation of the dissociation of acetone has been carried out in the intense laser regime. Castleman and coworkers[67−69] studied the photodissociation of acetone at intensity less than 10^{13} W/cm^2. The multiphoton effects in their studies initiated questioning whether ionization takes place followed by dissociation or vice versa. More interestingly, Levis et al.[70] reported strong-field optimal control of the photochemistry of

* To whom correspondence should be addressed. Tel: 86-10-62555347. Fax: 86-10-62563167. E-mail: Kong@mrdlab.icas.ac.cn.

† Permanent address: Chemistry Department, College of Science, Cairo University, Cairo, Egypt.

10.1021/jp026331a CCC: $25.00
Published on Web 12/07/2002

acetone. They demonstrated that the closed-loop learning process with a genetic algorithm is an efficient method for controlling photodissociation and ionization yields when strong-field excitation is employed. Furthermore, they showed that the mass spectrum of a molecule can be dramatically altered with tailored excitation pulse shapes.

In this paper, we report our experimental study on the dissociation of acetone in the rather moderate intensity regime of $10^{13}-10^{14}$ W/cm^2, in which the interesting reactions take place. We have found the stepwise, field-assisted dissociation mechanism, which cannot be explained by Coulomb explosion (taking place in very strong laser fields, $>10^{14}$ W/cm^2). The dissociation pattern is also different from that caused by multiphoton excitation (taking place in rather weak fields $<10^{12}$ W/cm^2) and conventional photodissociation (in a very weak field, $<10^7$ W/cm^2). Theoretically, we calculate the dissociation thresholds and predict the sequence of the dissociation pathways by increasing the laser intensity. We can then mimic the fragmentation pattern of polyatomic molecules in intense laser fields. We intend to provide our contribution to clarify the dissociation mechanism by combining experimental investigation and theoretical calculations. Therefore, we have proposed a model to explain the field-induced dissociation mechanism of acetone. The model had been successful in interpreting the dissociation of methane[41] and acetaldehyde.[42] A summary of the model is given in section III.

II. Experiment

The laser system used in this study was a home-built mode-locked femtosecond Ti:sapphire oscillator operating around 800 nm, which was pumped by a diode-pumped, frequency-doubled laser (532 nm, Verdi, Coherent). As a seed pulse, the 800 nm, 30 fs laser pulse from the oscillator was stretched and then led to a multipass Ti:sapphire laser amplifier (Quantronix, Odin), which was pumped by the second harmonic of a Nd:YLF laser. The amplified laser pulse was compressed to 160 fs detected by an autocorrelator, and the maximum energy output was about 300 μJ per pulse. The amplified femtosecond pulse was focused into the chamber of the linear time-of-flight (TOF) mass spectrometer (MS) by a 15 cm focal lens. The laser spot is assumed as a Gaussian distribution. The spot diameter of 37.5 μm is determined by the focal length (15 cm) times the beam divergence, which is measured as 0.25 mrad. The laser energy was monitored by a power meter (LPE-1B, Physcience Opto-electronics Co., Ltd., Beijing, China) at a repetition frequency of 1 kHz. The fluctuation of the averaged energy of 1000 laser pulses is 5% with the pulse-to-pulse fluctuation of 4% rms. The gaseous molecules were continuously effused into the chamber through an orifice with 500 μm with a background pressure of 7.2×10^{-7} Torr and acetone gas pressure of 4.6×10^{-6} Torr. The calculated number density under these conditions was 1.5×10^{11} cm^{-3}, a value showing negligible mass charge effects. The gas flow was crossed with the focused laser beam. The fragment ions produced in the laser beam were extracted by an electric field of 200 V passing through an aperture of 3 mm at 8 mm away from the laser beam. The ions were then accelerated by 900 V in a two-stage electric field and flew freely to a dual microchannel plate (MCP) through a 50 cm free-field flight tube. The ion signal was detected by the MCP and acquired by a 100 MHz high-speed transient recorder and then transferred to the computer for data acquisition.

III. The Model

There has been a lack of a suitable theoretical model to explain the field-assisted dissociation in the intensity regime of interest, $10^{13}-10^{14}$ W/cm^2, in which the chemical bond takes place. Because only singly charged ionized species are found in this moderate intensity, the Coulomb explosion model cannot interpret the dissociation process. Few models have been proposed to explain the dissociation of molecules in intense laser fields. One model is the "barrier suppression model", introduced by Dietrich and Corkum [71] to explain the dissociation of a strongly bound diatomic molecular ion. The second model, which is a modification of the above model, was proposed by Thachuck and Wardlaw.[72] It is applied for explaining the dissociation of a diatomic ion in an intense laser field using a one-dimensional model with a Morse function representing the nuclear interaction potential and coupling to a linear dipole moment representing the interaction with the laser field. They used classical trajectories to investigate some qualitative features of the dissociation process. The above two models were used for diatomic molecular ions only. The third model, which was based on the changes of the electron charge distribution, was proposed by Mathur and co-workers[73] to interpret the dissociation of polyatomic molecules.

To interpret the stepwise dissociation process of polyatomic molecules in intense laser fields, a simple model that can quantitatively interpret the dissociation dynamics of such molecules in strong fields of ultrashort laser pulse duration was proposed. The model will be described in detail elsewhere.[41] Briefly, the proposed model assumes that when the laser field is applied to a polyatomic molecule, only the change of one bond length, which lies along with the laser field, is taken into account and the rest of the molecular geometry is fixed. In that sense, the model can be considered as a quasi-diatomic model. Employing the model to explain the dissociation of a molecule consists of several calculations: potential energy surfaces of the ground state of the molecular ion at different field intensities (dressed PESs), quasi-classical trajectory (QCT) of the bond length with time, the dissociation probability, and the dissociation threshold intensities.

The model calculations started by optimizing the geometry of the neutral molecule and the molecular ion. The profile of the dissociative bond distance in the PESs of the ground state of the molecular ion has been calculated at different field intensities in the level of Hartree−Fock (RHF or UHF)/6-31G, with the "FIELD" option in the Gaussian 98 package.[74] In the ion, the dissociative bond is chosen to set parallel to the electric field vector of the applied laser and calculating the ground-state PESs profile of the ion at different field intensities and with two opposite directions of the electric field along the dissociative bond axis. This step gives a set of the dressed ground-state PESs.

The dissociation dynamics of the molecular ion can be considered as the dissociative bond is pulled off by the laser field, where the nuclear motion can be represented by the motion of a Gaussian wave packet taking place on a ground dressed PES modulated by the oscillating optical field. The wave packet moves periodically through various dressed PESs with different laser intensities in one optical cycle. For the laser wavelength of 800 nm, the width of an optical cycle is 2.7 fs. The 100 fs laser pulse accordingly contains 37 cycles.

To obtain the variation in the bond lengths of the molecular ions, thousands of trajectories reflect the change of the dissociating bond with time. The change of the dissociating bond with time is obtained by averaging these trajectories. In a strong field, the bond distance monotonically increases; the dissociation probability was defined as the ratio of the weighted number of the dissociative trajectories leading to the total number of

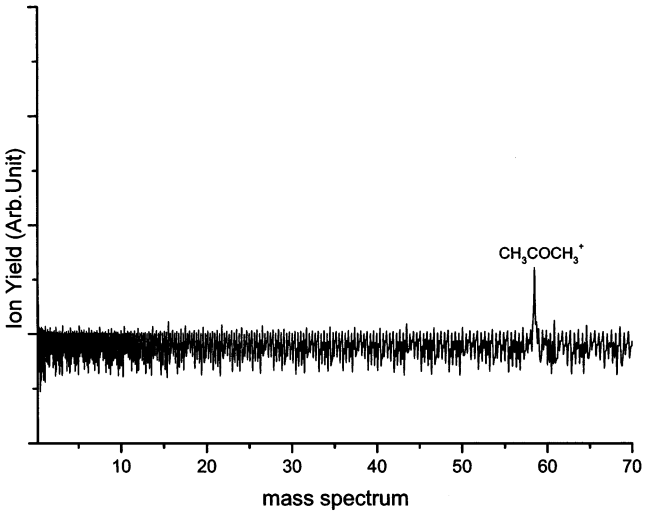

Figure 1. The mass spectrum of acetone at the laser intensity of 0.4 $\times$ 10^{14} W/cm^2 using 160 fs laser pulses at 800 nm and a gas pressure of 4.6 $\times$ 10^{-6} Torr. Only the parent ion, $CH_3COCH_3^+$, appears.

trajectories. Threshold laser intensity can be defined as that intensity for which in 100 fs the laser field causes 1% of the weighted trajectories to reach 6 Å. A bond distance of 6 Å can be considered as the critical distance for dissociation.

IV. Results and Discussions

1. Mass Spectra at Different Laser Intensities. The stepwise dissociation of acetone in the moderate intensity regime 10^{13}−10^{14} W/cm^2 has been experimentally studied using 160 fs laser pulses. To verify the stepwise dissociation, a series of TOF mass spectral measurements for detecting the parent ions and the primary and the secondary fragment ions formed at different laser intensities were conducted. The ions formed were monitored as the intensity was gradually increased. Only singly charged ions have been identified in this intensity regime. There was no evidence for multiply charged ions.

At relatively low intensity of 0.4 $\times$ 10^{14} W/cm^2, only the parent ion $CH_3COCH_3^+$ (58 amu) is observed, as shown in Figure 1. The intensities beyond this intensity are marked as three levels from I to III, corresponding to 0.72 $\times$ 10^{14}, 0.96 $\times$ 10^{14}, and 1.1 $\times$ 10^{14} W/cm^2, respectively. At level I of the laser intensity (0.72 $\times$ 10^{14} W/cm^2), the primary fragment ions CH_3^+ (15 amu) and CH_3CO^+ (43 amu) are observed, as shown in Figure 2a. This fact indicates that the C−C bond starts to break at the level I of laser intensities. It was noticed that although the dissociation of a singly charged ion as $CH_3COCH_3^+$ directly yields a pair of charged and neutral species, like CH_3^+ and CH_3-CO or CH_3 and CH_3CO^+, both the ions CH_3^+ and CH_3CO^+ appear in the same spectrum, because the threshold of the field-assisted ionization is normally lower, about 10^{13} W/cm^2. The neutral fragment can soon ionize. With an increase of the laser intensity to level II (0.96 $\times$ 10^{14} W/cm^2), new peaks have been identified. The $CH_3CCH_3^+$ (42 amu) and the O^+ (16 amu) ions were identified, as shown in Figure 3a. This observation implies that the C═O bond of the parent ion is dissociating at this laser intensity. The O^+ does not result from the CH_3CO^+ because CH_3C^+ (27 amu) was not found. Upon further increase of the laser intensity to reach level III (1.1 $\times$ 10^{14} W/cm^2), we observed the appearance of new peaks in the mass spectrum. The H^+ (1 amu) was identified and is shown in Figure 4a, implying the dissociation of the C−H bond. In addition, two peaks have appeared at 27 and 14 amu, from which we have assigned the former to be CH_3C^+ ion and the latter to be the CH_2^+ ion.

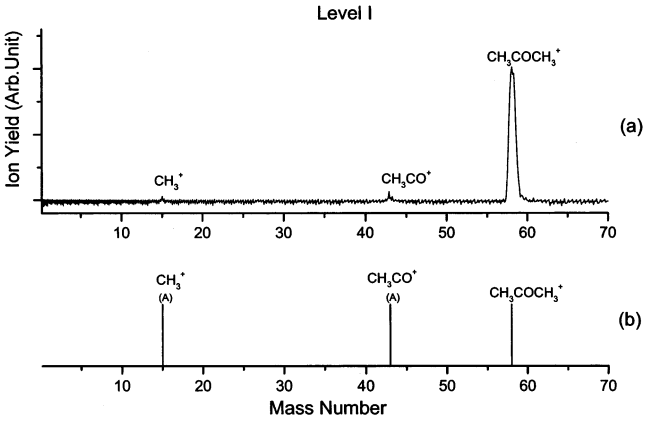

Figure 2. The (a) experimental mass spectrum of the dissociation of acetone at the laser intensity of 0.72 $\times$ 10^{14} W/cm^2 (level I) using 160 fs laser pulses at 800 nm and a gas pressure of 4.56 $\times$ 10^{-6} Torr and (b) simulated mass spectrum of the dissociation of acetone at the threshold intensity of 2.2 $\times$ 10^{14} W/cm^2 (level I). The simulated mass spectrum reproduces the experimental mass spectrum at this intensity. The dissociation channel refers to channel A in Chart 1.

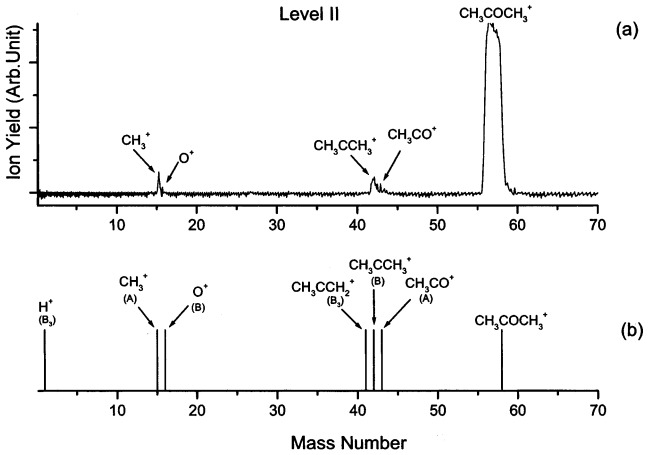

Figure 3. The (a) experimental mass spectrum of the dissociation of acetone at the laser intensity of 0.96 $\times$ 10^{14} W/cm^2 (level II) using 160 fs laser pulses at 800 nm and a gas pressure of 4.6 $\times$ 10^{-6} Torr and (b) simulated mass spectrum of the dissociation of acetone at the threshold intensity of 2.3 $\times$ 10^{14} W/cm^2 (level II). The simulated mass spectrum reproduces the experimental one. The dissociation channels refer to the channels A, B, B_2, B_3, or C_6 in Chart 1.

Upon further increase of the laser intensity to 1.5 $\times$ 10^{14} W/cm^2, we have observed the products of dissociation of all primary and secondary channels. The identification of further dissociation channels is beyond the scope of this work, but the results strongly indicate and verify the stepwise nature of dissociation of acetone in the intensity 10^{13}−10^{14} W/cm.

2. Theoretical Calculations on the Dissociation Dynamics. Theoretically, the quasi-diatomic model has successfully been used to assign the different dissociation channels and their products in the experimental observations. Here, we study the dissociation of acetone using three levels of intensities labeled I−III. Calculations of the field-affected PESs are first made for the C−C bond primary dissociation channel of the parent ion at different laser intensities and with different field directions, as shown in Figure 5a,b. The tendency for C−C bond dissociation is higher when the field is as indicated in Figure 5a. There are four different types of bonds in acetone, namely, the C−C bond, the C−O bond, the C−$H_{(1)}$, and the C−$H_{(2)}$, as displayed in the inset of Figure 6. The QCT of the dissociation process is shown in Figure 6, for which the calculation procedure was described in section III. All of the calculations in this work are

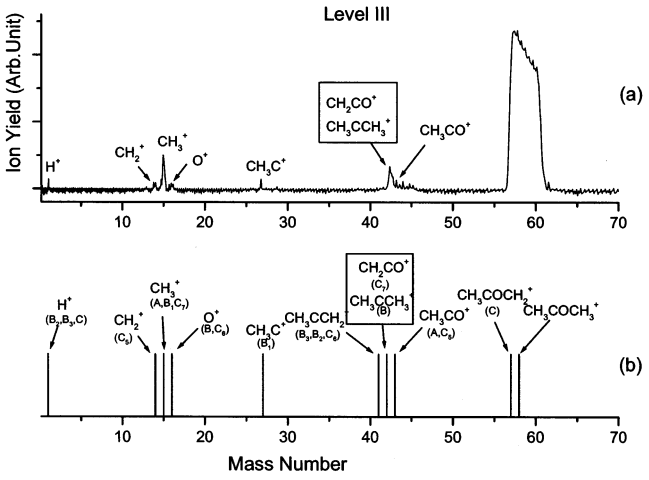

Figure 4. The (a) experimental mass spectrum of the dissociation of acetone at the laser intensity of 1.1×10^{14} W/cm^2 (level III) using 160 fs laser pulses at 800 nm and a gas pressure of 4.56×10^{-6} Torr and (b) simulated mass spectrum of the dissociation of acetone at the threshold intensity of 2.5×10^{14} W/cm^2 (level III). The simulated mass spectrum reproduces the experimental mass spectrum via channels A, B, C, B_1, B_2, B_3, and C_6.

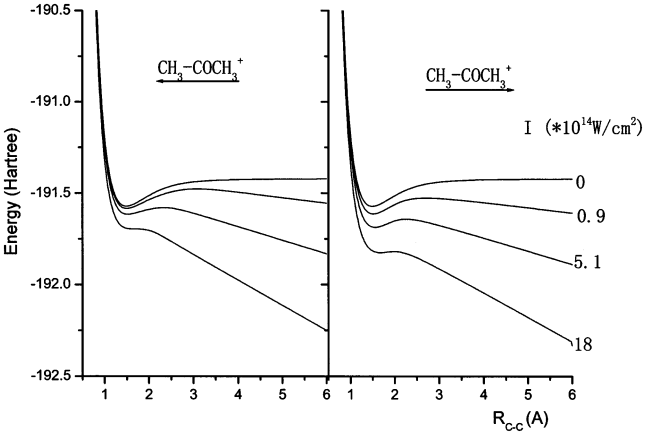

Figure 5. The PES of the C−C bond dissociation of the parent ion $CH_3COCH_3^+$ with the laser field vector direction indicated by the arrow (a) from the CH_3 group to the CH_3CO group or (b) from the CH_3CO group to the CH_3 group.

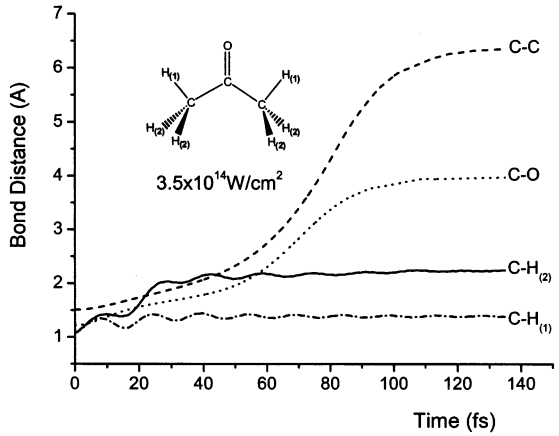

Figure 6. Trajectory of the dissociation of the different bonds of acetone at the intensity of 3.5×10^{14} W/cm^2. The numbering of the H atoms of the different C−H bonds is shown in the inset of the figure.

based on the fact that the laser polarization vector is parallel to each dissociative bond axis. The results show that for the same laser intensity of 3.5×10^{14} W/cm^2 and at a certain time interval (for example, 100 fs) the average C−C bond distance shows the highest elongation, reaching to 6 Å and hence complete bond dissociation, while the CO, C−$H_{(1)}$, and C−$H_{(2)}$ bonds show much smaller elongation, and hence lower dissociation tendency, at the same intensity. The results explain why we only observed the fragments CH_3^+ and CH_3CO^+ ions at the level I (the threshold intensity of 2.2×10^{14} W/cm^2 corresponding to 1% dissociation) of laser intensity, as shown in Figure 2b.

The simulation of the dissociation at the level II (laser intensity of 4.2×10^{14} W/cm^2) predicts that the dissociation of the C−O bond in the parent ion is completed, giving $CH_3CCH_3^+$ and O^+ fragments. The threshold intensity of 1% dissociation is calculated as 2.3×10^{14} W/cm^2, and the dissociation pattern is shown in Figure 3b. Figure 4b shows the simulated mass spectrum at the level III laser intensity. According to our theoretical calculations, the threshold intensity of the C−H bond breaking is 2.5×10^{14} W/cm^2, while the $CH_3COCH_3^+$ seriously dissociates at a laser intensity of 5.1×10^{14} W/cm^2 resulting in the formation of $CH_3COCH_2^+$ and $H_{(2)}^+$ as the primary fragment ions. By using the above theoretical model, we have also calculated the dissociation probabilities of different secondary dissociation channels at the level III. The processes refers to the secondary dissociation of $CH_3CCH_3^+$ and $CH_3COCH_2^+$ leading to the formation of the experimentally observed products $CH_3C^+ + CH_3^+$, $CH_3CCH_2^+ + H_{(1)}^+$, and $CH_2^+ + CH_3CO^+$, respectively.

At the intensity higher than level III, more secondary dissociation channels can take place, mostly giving H^+ ions. The dissociation of CH_3CO^+ leading to the formation of the products $CH_2CO^+ + H^+$ and $CH_3^+ + CO^+$ is verified by the calculations. The dissociation of $CH_3COCH_2^+$ leads to the formation of the products $CH_3COCH^+ + H_{(1)}^+$, $CH_2COCH_2^+ + H_{(3)}^+$, and $CH_2COCH_1^+ + H_{(4)}^+$, respectively.

The simulated dissociation pattern was in a very good agreement with the TOF mass spectra at all of the levels of laser intensities. However, it must be noticed that the experimental threshold intensity, at which the fragment ions start to appear, is rather lower compared to the theoretical threshold intensities. The QCT calculations show that by adopting a value of 1% of the calculated fragment ion yield as a criterion of the "theoretical threshold intensity", the values of the theoretical threshold intensities and the experimental threshold intensities are quite close. For example, the values of the theoretical threshold intensities of 2.2×10^{14}, 2.3×10^{14}, and 2.5×10^{14} W/cm^2 correspond to those observed "experimental" threshold intensities of 0.72×10^{14}, 0.96×10^{14}, and 1.1×10^{14} W/cm^2 for the dissociation of the C−C, C−O, and C−$H_{(1)}$ bonds, respectively.

3. The Correlation between the Experimental and the Calculated Results. The agreement between the theoretical predictions and the experimental observations makes it possible to interpret the entire dissociation process. To correlate the experimental and theoretical intensities, the theoretical predictions of the dissociation threshold (as simulated patterns) and the experimental inspection of the mass spectral patterns were combined. The results are shown with Chart 1. The chart clearly illustrates the stepwise dissociation mechanism.

Below the lowest level of laser intensity, level I, only the parent ion is observed, showing that none of the chemical bonds can be cracked. In Chart 1, the dissociation of the C−C, C−O, C−$H_{(2)}$, and C−$H_{(1)}$ bonds is marked as A, B, C, and D, respectively. It was found that the C−C bond dissociates first in the intensity level I giving the primary fragment ions CH_3^+ and CH_3CO^+, shown as dissociation channel A. It was also

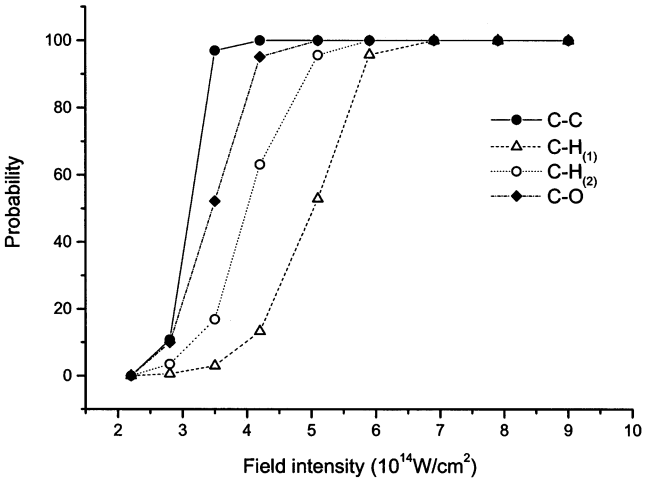

Figure 7. The dissociation probability of the different bonds of acetone at different field intensities.

CHART 1: The Possible Primary and Secondary Dissociation Channels of the Parent Ion, $CH_3COCH_3^+$, Shown with the Experimental and Theoretical Levels I−IV of Laser Intensity

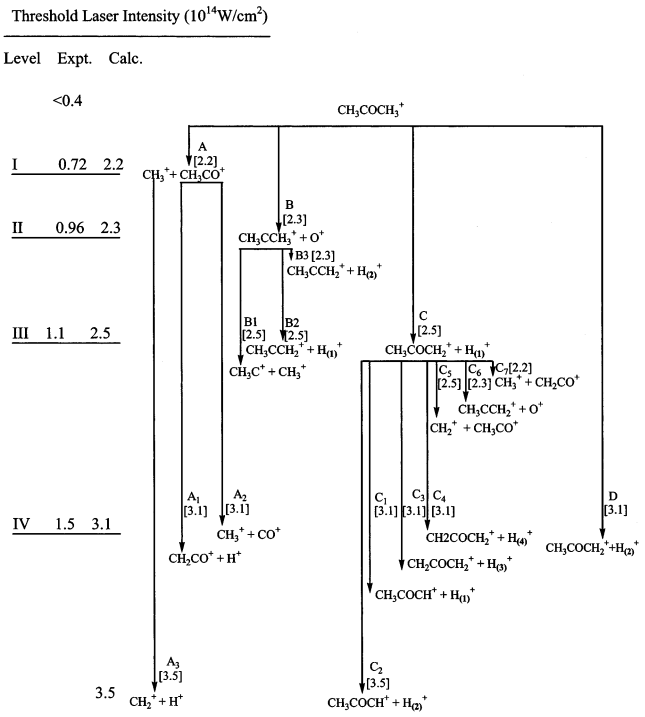

found that increasing the laser intensity to the level II leads to another dissociation channel, the C═O bond dissociation channel (channel B), giving rise to the $CH_3CCH_3^+$ and O^+ primary ions. A further increase of the intensity to the level III results in a third dissociation channel, namely, the C−$H_{(1)}$ bond channel C. This gives rise to the formation of the primary dissociation products $CH_3COCH_2^+$ and $H_{(1)}^+$. Increasing the laser intensity to the level IV results in the formation of the primary fragment ions $CH_3COCH_2^+ + H_{(2)}^+$ (channel D), in addition to all of the primary channels detected at lower intensities, A, B, and C. This is further verified by the dissociation probability calculations shown in Figure 7, in which the dissociation probabilities of the different bonds of acetone at different laser intensities were displayed. In the low-intensity region and for the same laser intensity, the C−C bond shows the highest dissociation probability, higher than that of the CO, while the C−$H_{(2)}$ and C−$H_{(1)}$ bonds show the lowest dissociation probability.

The secondary dissociation channels are presented in Chart 1. For the further dissociation of CH_3^+ and CH_3CO^+ ions, three channels have been found in relatively high intensities. At the level IV of laser intensity, CH_3CO^+ ion may undergo two dissociation paths, A_1 or A_2, leading to the formation of $CH_2CO^+ + H^+$ or $CH_3^+ + CO^+$, respectively. The dissociation of CH_3^+ ion to $CH_2^+ + H^+$, channel A_3, requires even higher intensity. The secondary dissociation of $CH_3CCH_3^+$ ion occurs at lower laser intensities; the cracking of the C−C bond, channel B_1, and the C−$H_{(1)}$, channel B_2, bond takes place at the level III. Another H-elimination process, breaking the C−$H_{(2)}$ bond, channel B_3, even starts at the level II. In contrast, the H-elimination from $CH_3COCH_2^+$ (channels C, C_2, C_3, and C_4) is difficult, only occuring at the level IV, while cracking the C−C bond, channels C_5 and C_7, or cracking the C−O bond, channel C_6, happen at lower intensity, the level III.

V. Conclusion

The field-assisted dissociation of acetone cation has been studied at the laser intensities of $10^{13}-10^{14}$ W/cm^2. A TOF-MS is used to detect the fragments of the dissociation. Gradually increasing the laser intensity from level I to level III, we have observed the singly charged species in the order of the parent (below level I), CH_3^+ and CH_3CO^+ (at level I), $CH_3CCH_3^+$ and O^+ (at level II), CH_3C^+, $CH_3CCH_2^+$, and $CH_3COCH_2^+$ (at level III), and smaller ions (beyond level III). No doubly or multiply charged ionic species were found. These facts verify the stepwise dissociation mechanism of the acetone ion. The quasi-diatomic model of the field-assisted dissociation of polyatomic molecules has been used for explaining the dissociation mechanism. QCT calculations have been performed on each bond cracking process. The calculated threshold intensities of the dissociation show the feasibility of the bond breaking in the order C−C, C−O, C−H (in the parent ion), C−C, and C−H (in the $CH_3CCH_3^+$ primary ion), which is in good agreement with the results of the mass spectra at the different levels of the laser intensity. The above facts verify that in the moderate laser intensity ($10^{13}-10^{14}$ W/cm^2), the dissociation mechanism is completely different from the conventional photolysis model, the multiphoton excitation model, and the Coulombic explosion model. In contrast, the field-assisted quasi-diatomic dissociation model successfully explains the stepwise process.

The outcome of this study is to utilize the mechanism of molecular dissociation at that intensity in pursuing more elaborate studies of quantum controlling of the products of chemical reactions, an active area of research. One of the exciting experiments is controlling the ratio of reaction channels for a derivative molecule of acetone by femtosecond intense laser pulse.[70] The present work may elucidate the mechanism of the laser controlling, the strong field effects on the dissociation probability of the competing channels via changing laser intensity, pulse duration, or pulse chirp.

Acknowledgment. We thank Professor Andong Xia for the help and assistance in running the laser system. We also thank the National Supercomputing Center of China, Beijing, for the allocated computer time for the computational work performed. One of us, M. Elshakre, thanks the TWAS, south-south scheme, for the research fellowship. He also thanks the Institute of Chemistry, Chinese Academy of Science, for the hospitality and the generous resources that made his stay enjoyable in China.

References and Notes

(1) Bandrauk, A. B. *Molecules in Laser Fields*; Dekker: New York, 1994.

(2) Codling, K.; Frasinski, L. J. *J. Phys. B: At., Mol. Opt. Phys.* **1993**, *26*, 783.

(3) Corkum, P. B.; Dietrich, P. *Comments At. Mol. Phys.* **1993**, *28*, 357.

(4) Guisti-Suzor, A.; Mies, F. H.; DiMauro, L. F.; Charron, E.; Yang, B. *J. Phys. B: At., Mol. Opt. Phys.* **1995**, *28*, 309.

(5) Ilkov, F. A.; Walsh, T. D. G.; Turegon, S.; Chin, S. L. *Phys. Rev. A.* **1995**, *51*, 2695.

(6) Bucksbaum, P. H.; Zavriyev, A.; Muller, H. G.; Schumacher, D. W. *Phys. Rev. Lett.* **1990**, *64*, 1883.

(7) Decker, J. E.; Xu, G.; Chin, S. L. *J. Phys. B*: *At., Mol. Opt. Phys.* **1991**, *24*, L281.

(8) Ellert, Ch.; Stapelfeldt, H.; Constant, E.; Sakai, H.; Wright, J.; Rayner, D. M.; Corkum, P. B. *Philos. Trans. R. Soc. London, Ser. A* **1998**, *356*, 329.

(9) Iwamae, A.; Hishikawa, A.; Yamanouchi, K. *J. Phys. B: At., Mol. Opt. Phys.* **2000**, *33*, 223−240.

(10) Chelkowski, S.; Bandrauk, A. D. *J. Phys. B: At., Mol. Opt. Phys.* **1995**, *28*, L723−L731.

(11) Ledingham, K. W. D.; Smith, D. J.; Singhal, R. P.; McCanny, T. C.; Graham, P.; Kilick, H. S.; Peng, W. X.; Langley, A. J.; Taday, P. F.; Kosmidis, C. *J. Phys. Chem. A* **1999**, *103*, 2952−2963.

(12) Larsen, J. J.; W.-Larsen, I.; Stapelfeldt, H. *Phys. Rev. Lett.* **1999**, *83* (6), 1123−1126.

(13) Larsen, J. J.; Hald, K.; Bjerre, N.; Stapelfeldt, H. *Phys. Rev. Lett.* **2000**, *85* (12), 2470−2473.

(14) Sakai, H.; Safvan, C. P.; Larsen, J. J.; HilligsØe, K. M.; Hald, K.; Stapelfeldt, H. *J. Chem. Phys.* **1999**, *110* (21), 10235.

(15) Larsen, J. J.; Sakai, H.; Safvan, C. P.; W.-Larsen, I.; Stapelfeldt, H. *J. Chem. Phys.* **1999**, *111* (17), 7774−7781.

(16) Cornaggia, C.; Herring, Ph. *Phys. Rev. A* **2000**, *62*, 023403.1−023403.13.

(17) Cornaggia, C. *Phys. Rev. A* **1995**, *52*, R4328−R4331.

(18) Hering, Ph.; Cornaggia, C. *Phys. Rev. A* **1998**, *57* (6), 4572−4580.

(19) Cornaggia, C.; Normand, D.; Morellec, J. *J. Phys. B: At., Mol. Opt. Phys.* **1992**, *25*, L415−L422.

(20) Mathur, D.; Safvan, C. P.; Kumar, G. R.; Krishnamurthy, M. *Phys. Rev. A.* **1994**, *50*, R7−R9.

(21) Bhardwaj, V. R.; Vijayalakshmi, K.; Mathur, D. *Phys. Rev. A* **1999**, *59* (2), 1392−1398.

(22) Vijayalakshmi, K.; Bhardwaj, V. R.; Mathur, D. *J. Phys. B: At., Mol. Opt. Phys.* **1997**, *30*, 4065−4085.

(23) Bhardwaj, V. R.; Vijayalakshmi, K.; Mathur, D. *Phys. Rev. A* **1997**, *56* (3), 2455−2458.

(24) Castillejo, M.; Couris, S.; Koudomas, E.; Martin, M. *Chem. Phys. Lett.* **1999**, *308*, 373−380.

(25) Castillejo, M.; Couris, S.; Koudomas, E.; Martin, M. *Chem. Phys. Lett.* **1998**, *289*, 303−310.

(26) Ledingham, K. W. D.; Singhal, P. R.; Smith, D. J.; McCanny, T.; Graham, P.; Kilic, H. S.; Peng, W. X.; Wang, S. L.; Langley, A. J.; Taday, P. F.; Kosmidis, C. *J. Phys. Chem. A* **1998**, *102*, 3002−3005.

(27) Smith, D. J.; Ledingham, K. W. D.; Kilic, H. S.; McCanny, T.; Peng, W. X.; Singhal, R. P.; Langley, A. J.; Taday, P. F.; Kosmidis, C. *J. Phys. Chem. A* **1998**, *102*, 2519−2526.

(28) Kosmidis, C.; Ledingham, K. W. D.; Kilic, H. S.; McCanny, T.; Singhal, R. P.; Langley, A. J.; Shaikh, W. *J. Phys. Chem. A* **1997**, *101*, 2264−2270.

(29) Tzallas, P.; Kosmidis, C.; Ledingham, K. W. D.; Singhal, R. P.; McCanny, T.; Graham, P.; Hankin, S. M.; Taday, P. F.; Langley, A. J. *J. Phys. Chem. A* **2001**, *105*, 529−536.

(30) Ledingham, K. W. D.; Singhal, R. P. *Int. J. Mass Spectrom. Ion Processes*, **1997**, *163*, 149−168.

(31) Wu, C. Y.; Ren, H. Z.; Liu, T. T.; Ma, R.; Yang, H.; Hongling, J.; Gong, Q. H. *J. Phys. B: At., Mol. Opt. Phys.* **2002**, *35*, 1−8.

(32) Kumar, G. R.; Safvan, C. P.; Rajgara, F. A.; Mathur, D. *J. Phys. B: At., Mol. Opt. Phys.* **1994**, *27*, 2981−2991.

(33) Cornaggia, C.; Schmidt, M.; Normand, D. *J. Phys. B: At., Mol. Opt. Phys.* **1994**, *27*, L123−L130.

(34) Cornaggia, C.; Solin, F.; Leblanc, C. *J. Phys. B: At., Mol. Opt. Phys.* **1996**, *29*, L749−L754.

(35) Safvan, C. P.; Thomas, R. V.; Mathur, D. *Chem. Phys. Lett.* **1998**, *286*, 329−335.

(36) Safvan, C. P.; Bhardawaj, V. R.; Kumar, G.; Mathur, D.; Rajgara F. A. *J. Phys. B: At., Mol. Opt. Phys.* **1996**, *29*, 3135−3149.

(37) Banerjee, V. R.; Kumar, G. R.; Mathur, D. *J. Phys. B: At., Mol. Opt. Phys.* **1999**, *32*, 4277−4292.

(38) Bhardwaj, V. R.; Vijayalakshmi, K.; Rajgara, F. A.; Mathur, D. *J. Phys. B: At., Mol. Opt. Phys.* **1999**, *32*, 1087−1095.

(39) Banerjee, S.; Kumar, G. R.; Mathur, D. *Phys. Rev. A* **1999**, *60* **(**5), R3369−R3372.

(40) Safvan, C. P.; Vijaylakshmi, K.; Rajgara, F. A.; Kumar, G. R.; Mathur, D. *J. Phys. B: At., Mol. Opt. Phys.* **1996**, *29*, L481−L487.

(41) Wang, S. F.; Gao, L. R.; Tang, X. P.; Elshakre, M. E.; Kong, F. A. *J. Phys. Chem.*, submitted for publication.

(42) Elshakre, M. E.; Gao, L. R.; Tang, X. P.; Wang, S. F.; Kong, F. A., to be submitted for publication.

(43) MacNeil, K. A. G.; Futrell, J. H. *J. Phys. Chem.* **1972**, *76*, 409.

(44) Hanckock, G.; Wilson, K. R. *Proceedings of the 4th International symposium on Molecular Beams (Peymeinada, Cannes, France)*; 1973.

(45) Lee, K. E. C.; Rice, S. R. *Adv. Photochem.* **1980**, *12*, 1.

(46) Baba, M.; Shinohara, H.; Nishi, N.; Hirota, N. *Chem. Phys.* **1984**, *83*, 221.

(47) Zuckermann, H.; Schmitz, B.; Haas, Y. *J. Phys. Chem.* **1989**, *93*, 4083.

(48) Donaldson, D. J.; Leone, S. R. *J. Chem. Phys.* **1986**, *85*, 817.

(49) Gaines, G. A.; Donaldson, D. J.; Strickler, S. J.; Vaida, V. *J. Phys. Chem.* **1988**, *92*, 2762.

(50) Donaldson, D. J.; Gaines, G. A.; Vaida, V. *J. Phys. Chem.* **1988**, *92*, 2766.

(51) Trentelman, K. A.; Kable, S. H.; Moss, D. B.; Houston, P. L. *J. Chem. Phys.* **1989**, *91*, 7498. Strauss, C. E. M.; Houston, P. L. *J. Chem. Phys.* **1990**, *94*, 8751.

(52) Gedanken, A.; McDiarmid, R. *J. Chem. Phys.* **1990**, *92*, 3237.

(53) McDiarmid, R.; Sabljic, A. *J. Chem. Phys.* **1988**, *89*, 6086.

(54) McDiarmid, R. *J. Chem. Phys.* **1991**, *95*, 1530.

(55) Brint, P.; O'Toole, L.; Couris, S.; Jordine, D. *J. Chem. Soc., Faraday Trans.* **1991**, *87*, 2891.

(56) O'Toole, L.; Brint, P.; Kosmidis, C.; Boulakis, G.; Tsekeris, P. *J. Chem. Soc., Faraday Trans.* **1991**, *87*, 3343.

(57) Phillis, J. G.; Goodman, L. *J. Chem. Phys.* **1993**, *98*, 3795.

(58) Woodbridge, E. L.; Fletcher, T. R.; Leone, S. R. *J. Phys. Chem.* **1988**, *92*, 5387.

(59) Hall, G. E.; Bout, D. V.; Sears, T. J. *J. Chem. Phys.* **1991**, *94*, 4182.

(60) North, S. W.; Blank, D. A.; Gezelter, J. D.; Longfellow, C. A.; Lee, Y. T. *J. Chem. Phys.* **1995**, *102*, 4447.

(61) Kim, S.; Pedersen, S.; Zewail, A. H. *J. Chem. Phys.* **1995**, *103* (1), 477.

(62) Xing, X.; McDiarmid, R.; Phillis, J. G.; Goodman, L. *J. Chem. Phys.* **1988**, *99*, 7565.

(63) Noyes, W. A., Jr. *Photochemistry and reaction kinetics*; Cambridge University Press: Cambridge, U.K., 1967; see also references therein.

(64) Turro, N. J. *Modern molecular photochemistry*; Benjamin/Cummings: Menlo Park, CA, 1978.

(65) Owrutsky, J. C.; Baronavski, A. P. *J. Chem. Phys.* **1998**, *108* (16), 6652−6659.

(66) Li, H.; Li, Q.; Mao, W.; Zhu, Q.; Kong, F. *J. Chem. Phys.* **1997**, *106* (14), 5943−5946.

(67) Buzza, S. A.; Snyder, E. M.; Castleman, A. W., Jr. *J. Chem. Phys.* **1996**, *104* (13), 5040−5047.

(68) Buzza, S. A.; Snyder, E. M.; Card, D. A.; Folmer, D. E.; Castleman, A. W., Jr. *J. Chem. Phys.* **1996**, *105* (17), 7425−7431.

(69) Zhong, Q.; Poth, L.; Castleman, A. W., Jr. *J. Chem. Phys.* **1996**, *110* (1), 192−196.

(70) Levis, R. J.; Menkir, G. M.; Rabitz, H. *Science* **2001**, *292*, 709−713.

(71) Dietrich, P.; Corkum, P. *J. Chem. Phys.* **1992**, *97* (5), 3187−3198.

(72) Thachuk, M.; Wardlaw, D. M. *J. Chem. Phys.* **1995**, *102* (19), 7462−7471.

(73) Vijayalakshmi, K.; Bhardwaj, V. R.; Mathur, D. *J. Phys. B: At., Mol. Opt. Phys.* **1997**, *30*, 4065−4085.

(74) Frisch, M. J.; Trucks, G. W.; Schlegel, H. B.; Scuseria, G. E.; Robb, M. A.; Cheeseman, J. R.; Zakrzewski, V. G.; Montgomery, J. A., Jr.; Stratmann, R. E.; Burant, J. C.; Dapprich, S.; Millam, J. M.; Daniels, A. D.; Kudin, K. N.; Strain, M. C.; Farkas, O.; Tomasi, J.; Barone, V.; Cossi, M.; Cammi, R.; Mennucci, B.; Pomelli, C.; Adamo, C.; Clifford, S.; Ochterski, J.; Petersson, G. A.; Ayala, P. Y.; Cui, Q.; Morokuma, K.; Malick, D. K.; Rabuck, A. D.; Raghavachari, K.; Foresman, J. B.; Cioslowski, J.; Ortiz, J. V.; Stefanov, B. B.; Liu, G.; Liashenko, A.; Piskorz, P.; Komaromi, I.; Gomperts, R.; Martin, R. L.; Fox, D. J.; Keith, T.; Al-Laham, M. A.; Peng, C. Y.; Nanayakkara, A.; Gonzalez, C.; Challacombe, M.; Gill, P. M. W.; Johnson, B. G.; Chen, W.; Wong, M. W.; Andres, J. L.; Head-Gordon, M.; Replogle, E. S.; Pople, J. A. *Gaussian 98*, revision A.7; Gaussian, Inc.: Pittsburgh, PA, 1998.